International Journal of Heat and Mass Transfer 52 (2009) 908–920

Contents lists available at ScienceDirect

International Journal of Heat and Mass Transfer

journal homepage: www.elsevier.com/locate/ijhmt

# Investigation of coated tubes in cross-flow boiling

Vikas J. Lakhera, Akhilesh Gupta *, Ravi Kumar

Department of Mechanical & Industrial Engineering, Indian Institute of Technology, Roorkee-247 667, Uttaranchal, India

ARTICLE INFO

*Article history:*
Received 28 September 2007
Received in revised form 28 May 2008
Available online 14 October 2008

*Keywords:*
Boiling heat transfer
Cross-flow
Surface roughness
Enhancement

ABSTRACT

The boiling in cross-flow is investigated for coated tubes (low-porosity, flame-sprayed) in this paper. The effect of surface roughness on flow boiling heat transfer for a horizontal tube surface in cross-flow is studied for saturated boiling of water at atmospheric pressure. The parameters varied were for flow velocity up to 3.24 kg/s ($G = 258.49$ kg/m$^2$ s), heat flux from 12 to 45 kW/m$^2$, surface roughness ($Ra$) from 0.3296 to 4.731 μm. Nominal enhancement in heat transfer coefficient at higher mass flux may be attributed to the continued nucleation at the uppermost surfaces (in the wake region of the flow) of the rougher tubes thereby increasing the overall heat transfer rate. The flow boiling data was found to best fit the Kutateladze asymptotic equation $h = h_l[1 + (h_{npb}/h_l)^n]^{1/n}$ with the value of $n = 2.258$ (which is close to the value of $n = 2$ suggested by Kutateladze).



## 1. Introduction

Cross-flow boiling is a common phenomena in a variety of industrial equipment such as kettle reboilers, flooded evaporators and chemical process equipment. Though the equipment comprises of tube bundles, the behaviour of a single tube in cross-flow boiling is of interest as that is a basic unit of a tube bundle.

For a single tube in boiling application, the pool boiling heat transfer coefficient is usually the governing factor in determining the overall heat transfer coefficients, and there is a lot of work done in this area specially the effect of heating surface conditions on the rate of heat transfer. Some of the earlier work includes those by Rohsenow [1], Hsu and Schmidt [2], Mostinski [3], Marto and Rohsenow [4], and Vachon et al. [5]. Cooper [6] quantitatively assessed the effect of surface roughness on pool boiling correlation. Thome [7] studied the nucleate boiling for two hydrocarbon mixtures on a GEWA-TX tube surface. Webb and Pais [8] provided a database for nucleate boiling data for five different surfaces using five different refrigerants at two saturation temperatures. Gorenflo [9] developed correlation for predicting nucleate pool boiling coefficients based on a reference heat transfer coefficient for a selection of fluids with consideration of surface roughness. Among the later works, Kang [10] and Pioro [11] studied the surface effects on pool boiling heat transfer.

Yilmaz and Westwater [12] studied the effect of velocity (2.4, 4 and 6.8 m/s) on the nucleate boiling heat transfer coefficient of R-113 outside a steam-heated copper tube in cross-flow and found that 'superposition' correlation as suggested by Rohsenow [13] worked well with the experimental results, i.e.,

$$q = q_{npb} + q_l \quad \text{or} \quad h = h_{npb} + h_l \tag{1}$$

Fand et al. [14] studied the forced convection boiling outside horizontal cylinders in cross-flow and found that the following asymptotic model suggested by Kutateladze [15] correlated well with the data for $n = 5.5$

$$\frac{h}{h_l} = \left[1 + \left(\frac{h_{npb}}{h_l}\right)^n\right]^{1/n} \tag{2}$$

Singh et al. [16] investigated the cross-flow boiling heat transfer over stainless steel tubes using R-12 at 362.5 kPa with velocity up to 3.1 mm s$^{-1}$ and found $n = 0.69$ in the Kutateladze equation to fit their data best.

Zukauskas and Karni [17] suggested the following correlation for predicting the single-phase average heat transfer coefficient from a cylindrical surface in cross-flow:

$$Nu_d = 0.27 Re_d^{0.6} \cdot \mathrm{Pr}^{0.37} \cdot \left(\frac{\mathrm{Pr}}{\mathrm{Pr}_s}\right)^{0.25} \tag{3}$$

The single-phase heat transfer coefficient ($h_l$) for rough cylinder in cross-flow was studied by Zukauskas and Ziugzda [18] and found that when roughness height is significantly smaller than thickness of velocity boundary layer, the velocity fluctuations induced by turbulence did not exert a perceptible effect on heat transfer. Also in the case of moderate roughness heights (~0.15 mm) the average heat transfer at subcritical Re increased insignificantly as compared with heat transfer from a smooth cylinder.

* Corresponding author.
*E-mail addresses:* vikasdme@iitr.ernet.in (V.J. Lakhera), akhilfme@iitr.ernet.in (A. Gupta), ravikfme@iitr.ernet.in (R. Kumar).

0017-9310/$ - see front matter © 2008 Elsevier Ltd. All rights reserved.
doi:10.1016/j.ijheatmasstransfer.2008.06.044

**Nomenclature**

| | |
|---|---|
| $A$ | heat transfer area, area (m$^2$) |
| $B$ | coefficient (dimensionless) |
| $d$ | diameter (m) |
| $G$ | mass flux (kg/(m$^2$ s)) |
| $h$ | heat transfer coefficient (W/(m$^2$ K)) |
| $I$ | current (A) |
| $k$ | thermal conductivity (W/(m K)) |
| $m$ | exponent (dimensionless) |
| $n$ | exponent (dimensionless) |
| $Nu$ | Nusselt number (dimensionless) |
| $P$ | pressure (bar) |
| $Pr$ | Prandtl number (dimensionless) |
| $q$ | heat flux (W/m$^2$) |
| $Q$ | power (W) |
| $Ra$ | surface roughness, average (μm, m) |
| $Re$ | Reynolds number (dimensionless) |
| $T$ | temperature (K, °C) |
| $V$ | voltage drop (V) |
| $\Delta T$ | wall superheat (K, °C) |

*Greek symbol*

| | |
|---|---|
| $\epsilon$ | enhancement ratio with respect to a plain surface (dimensionless) |

*Subscripts*

| | |
|---|---|
| d | based on tube diameter |
| f | bulk fluid |
| i | inner |
| l | convection |
| npb | nucleate pool boiling |
| o | outer |
| plain | based on plain tube |
| s | based on surface temperature |
| w | wall of test surface |
| wi | inner surface of tube/wall |
| wo | outer surface of tube/wall |

While the effect of surface roughness on increasing pool boiling heat transfer is well established from the references, it seems that enough work has not been carried out to study the effect of increased surface roughness under flow boiling. Thus, the present study was undertaken to determine the effect of surface roughness on flow boiling heat transfer outside the surface of a tubular surface. This study is an effort to investigate the potential of improving the thermal performance of heat exchangers using cross-flow boiling conditions.

## 2. Experimental setup

The experiments were performed using the setup shown schematically in Fig. 1. The principal components of the test loop include a test vessel, the test surface with heating arrangement, condenser, receiving tank, pump, preheater and measuring instruments with a data logging unit.

The test vessel was fabricated using a stainless steel sheet of 3 mm thickness and measured 570 mm × 165 mm × 200 mm. Two sides of the test vessel were provided with toughened glass in order to facilitate flow visualization and photography. One side of the test vessel was fitted with a 410 mm × 160 mm × 23 mm teflon sheet with 19.50 mm diameter holes drilled at required locations so that the test surface may be placed along with the required heating arrangement. The working fluid entered the vessel through a perforated, horizontal stainless steel sheet in order to facilitate flow uniformity at the entrance to the vessel. The vessel was fitted with a water level indicator and pockets to insert thermocouples/thermometer for measuring bulk fluid temperature. All the system components and pipings were well insulated using mineral wool insulation to prevent heat losses to the surroundings. The fluid entering the test vessel was saturated and its temperature was controlled using an electrically heated preheater with a variac control. The mixture of liquid and vapour from the test vessel entered into a storage cum condenser unit wherein a condenser was fitted on the upper portion. Cold water at a constant temperature was supplied to the condenser through a water chiller plant and the flow rate of cooling water was controlled through a valve. A pump of 0.745 kW was used to circulate the chilled water into the condensing unit.

The vapour produced in the evaporator (test vessel) was condensed in a condenser and recirculated from the receiver tank using a 3.728 kW (5 hp) pump. The fluid flow was regulated through gate valves and a by-pass line. The fluid flow rate was measured using a rotameter (for the lower mass flux range up to 60 kg/m$^2$ s) and an orifice (for the higher mass flux range 60–260 kg/m$^2$ s). The flow path between the rotameter and the orifice was regulated using a by-pass line and gate valves. The system pressure was monitored using a pressure gauge (0–6 kPa range).

The test surface (heater) was made up of stainless steel (AISI 304) tube having an outer diameter of 19.05 mm and a wall of 0.8 mm thickness with an effective heated length of 130 mm (Fig. 2). The tube was heated resistively by means of a high alternating current fed through a 15-kV A variable voltage transformer. The power supplied ($Q = V \times I$) to the test heater was measured using digital voltmeter (L.C. = 0.01 V) and digital ammeter (L.C. = 0.1 A). The heating arrangement is similar to one adopted by Gupta et al. [19].

The test tube inner wall temperature $T_{wi}$ was measured using eight T-type (copper constantan, 28 BWG) thermocouples evenly spaced at 45° interval on the tube inner wall and at midway between the heated length of the tube. A specially designed cylindrical fire clay probe (outer diameter ~7.4 mm) held the thermocouple beads firmly in place pressing against the inner wall of the test surface (as shown in Fig. 2). The bulk fluid temperature was measured using the average reading of four T-type thermocouples placed at suitable locations in the test vessel and in direct contact with the working fluid near the test surface. All the thermocouples were connected to a Keithley 2700 Data Acquisition System and temperatures recorded using Keithley XLINX software.

## 3. Experimental procedure

The heat transfer coefficient for the test surface was obtained using the equation

$$h = \frac{Q}{A(T_{wo} - T_f)} = \frac{q}{T_{wo} - T_f} \tag{4}$$

where $Q$ is the measured heating power ($Q = V \times I$) for the tube, $A$ is the total surface area of the tube, $T_{wo}$ is the outer wall temperature of the tube in contact with the boiling fluid and $T_f$ is the averaged bulk fluid saturation temperature.

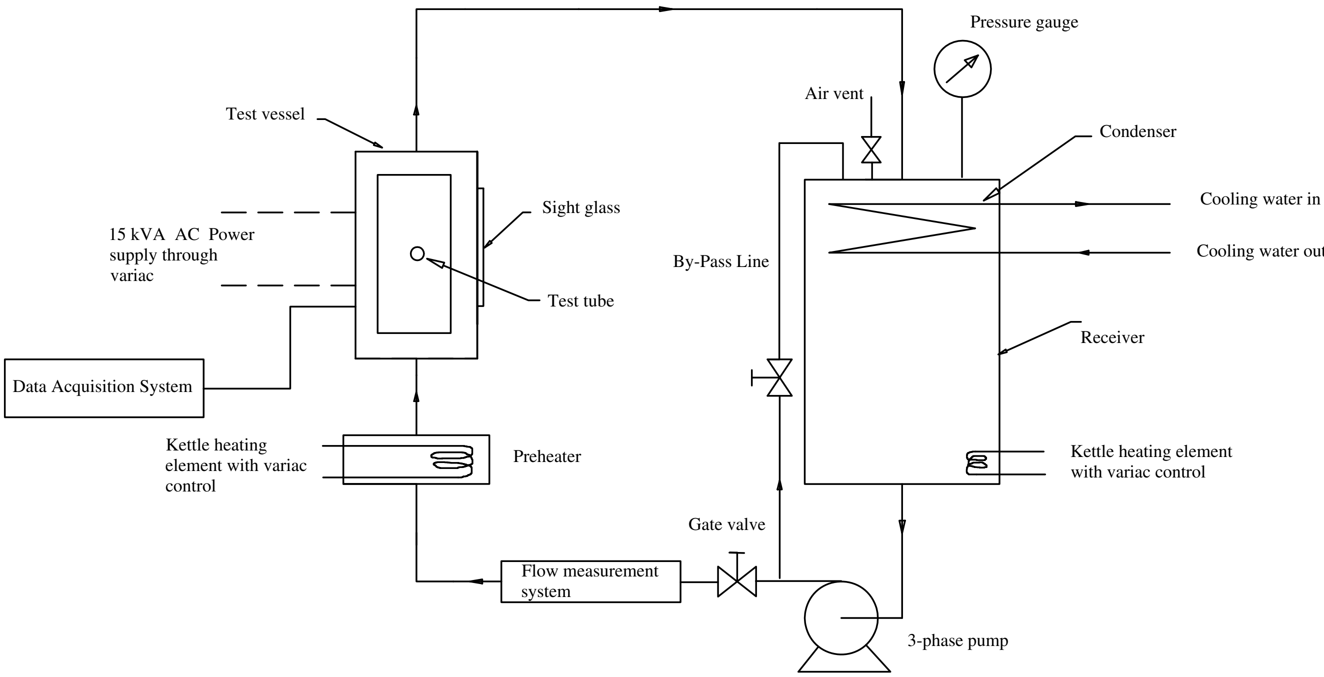


**Fig. 1.** A schematic of the experimental setup.

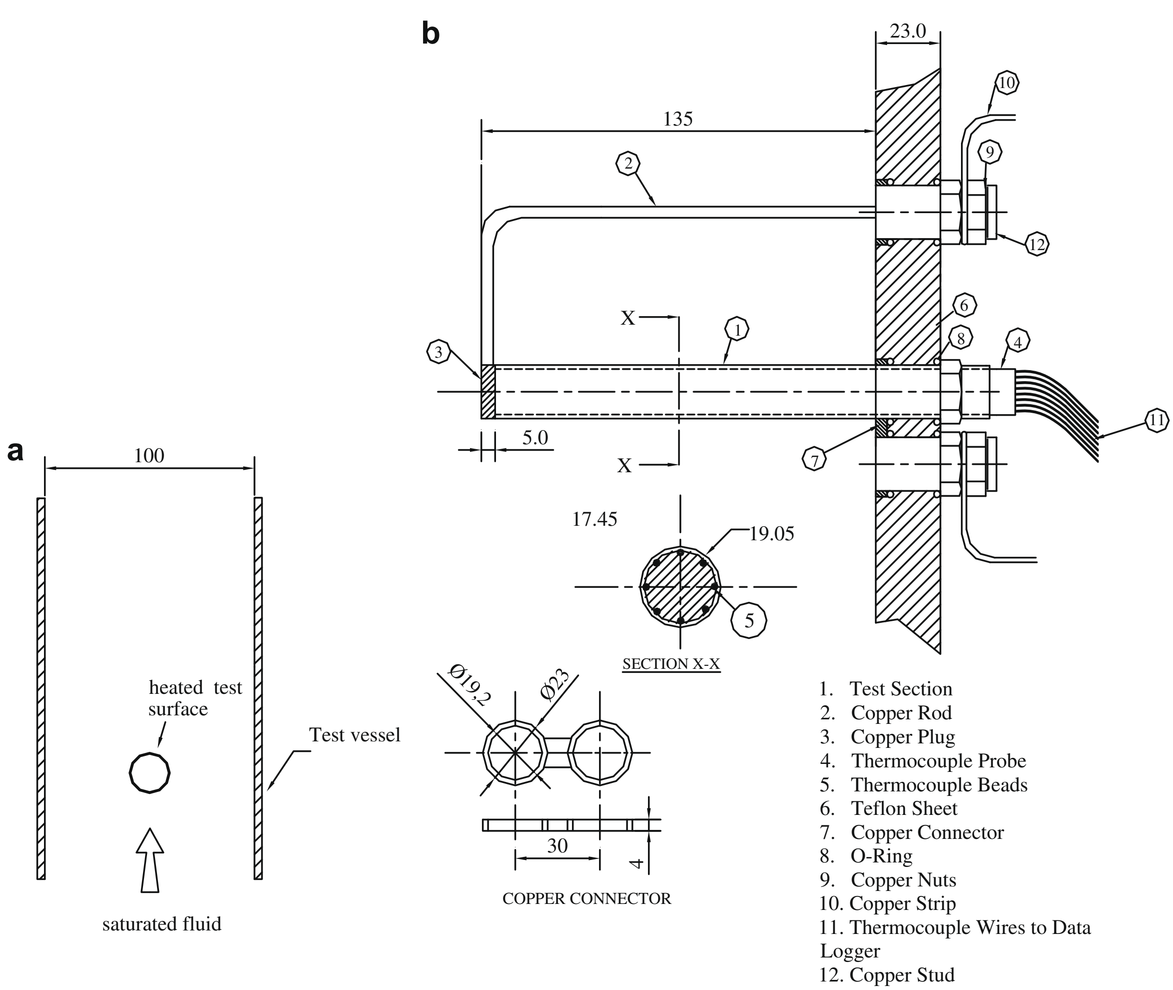


**Fig. 2.** Details of the test arrangement shown in (a), while the details of heater test surface, thermocouple position in the probe and the copper connector is shown in (b).

The temperature of the outer surface of the test tube $T_{wo}$ was estimated from the measured inner wall temperature $T_{wi}$ using the following relation

$$T_{wo} = T_{wi} + \frac{qd_o}{4k_w}\left[1 - \frac{2d_i^2}{d_o^2 - d_i^2}\ln\left(\frac{d_o}{d_i}\right)\right] \tag{5}$$

where $k_w$ is the thermal conductivity of the test surface material. The local heat transfer coefficient was then determined by using Eq. (4). The tube average heat transfer coefficient was obtained by averaging the eight local heat transfer coefficients.

Before the actual experiment was performed, the test tube was cleaned thoroughly and then heated at a constant heat flux of about 30 kW/m$^2$ for nearly 40 h spanned over one week interval in order to eliminate the starting effects and obtain reproducible results. In the initial stages of heating, the air vent provided at the top of the receiver tank was kept open and was closed only when steam in sufficient quantity started coming out thereby ensuring a complete air removal from the system. The system pressure during the experimentation was controlled within 1 ± 0.005 bar by adjusting the cooling water circulation rate in the condenser. The heat flux and the mass flux were adjusted to the desired levels and the data recorded only after the system attained a steady state. All experiments were performed with the heat flux being decreased in steps from the highest to the lowest values. At any heat flux under investigation, the experiments were performed with the mass flux being decreased from the highest ($G$ = 258.49 kg/m$^2$ s) to the lowest values ($G$ = 0). A similar procedure was adopted for each set of system and operating parameters for all the test surfaces investigated. For finding the single-phase heat transfer coefficient, the experiment was conducted by maintaining a steady fluid temperature and under different heat flux and mass flux conditions for a plain tube surface.

The test surface comprised of the plain surface of commercial finish and rough tubes of stainless steel (AISI 304) material. The rough tubes were created by thermal spraying plain stainless steel tube with a thin coating (0.08–0.125 mm thickness) of SS 316 on the outer surface using the wire flame process (wire diameter 3.15 mm). The porosity of the coatings formed was very low (<2%) and the roughness ($Ra$) of the test surface varied from 0.3296 to 4.731 μm (Table 1). The roughness ($Ra$) of the surface was measured with a Perthometer.

A scanning electron microscope (SEM) image of plain and rough tube surface (coated tube 2) is shown in Fig. 3 along with a cross-section of the rough tube showing the coating and the tube thicknesses.

The present study was undertaken in the range of system and operating parameters as follows:

| | |
|---|---|
| Working fluid: | distilled water |
| System pressure: | atmospheric (1 ± 0.005 bar) |
| Inlet fluid temperature: | saturation temperature |
| Heat flux range: | 12–45 kW/m$^2$ |
| Mass flux range: | 0–258.49 kg/m$^2$ s |
| Test surface: | plain stainless steel (AISI 304) tube with commercial finish. |
| : | roughened stainless steel tube (as per Table 1) |

The experimental uncertainties estimated through a propagation of error analysis for a typical set of data using methods described by Kline and McClintock [20] were found to be: $T$, ±0.2 °C; $q$, ±1.84%; $G$, ±2.52%; $h$, ±3.26%; $P$, 0.5 kPa; $Ra$, 12 nm.

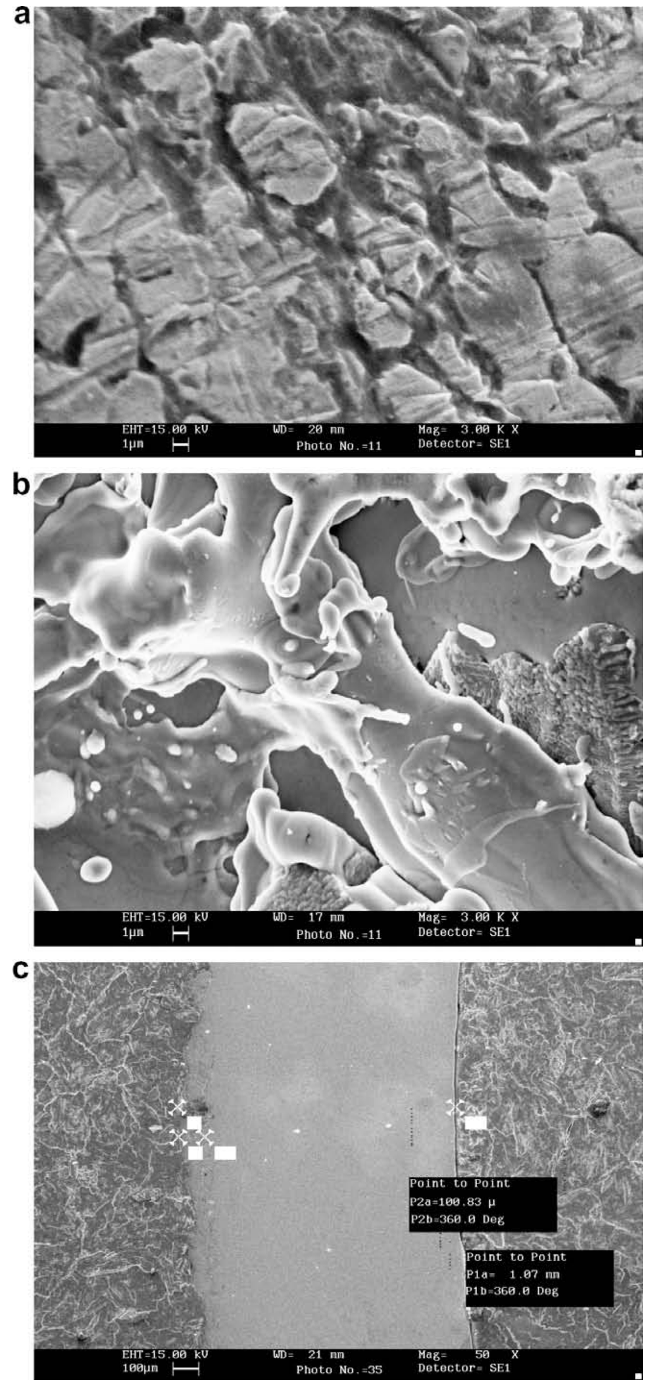


**Fig. 3.** SEM image for the test surfaces: (a) for a plain tube; (b) for rough tube 2; (c) cross-section image for test surface 2 showing coating thickness.

## 4. Results and discussion

The experimental results for the tube surfaces were analyzed and it was found that the increase in surface roughness increased the boiling heat transfer coefficient for the surface with an increase in heat flux at most of the mass flux values.

### 4.1 Single-phase heat transfer coefficient ($h_l$)

The single-phase experimental heat transfer coefficient for the plain tube surface was obtained at different heat flux conditions and varying the mass flux. The experimental results compared to

**Table 1**
Details of test surface

| Sr. No. | Test surface | Coating material/process | Tube o.d. (mm) | Coating thickness (mm) | Surface roughness, *Ra* (μm) |
|---|---|---|---|---|---|
| 1. | Plain tube | – | 19.05 | – | 0.3296 |
| 2. | Coated tube 1 | S.S/wire flame | 19.21 | 0.08 | 2.627 |
| 3. | Coated tube 2 | S.S/wire flame | 19.25 | 0.10 | 3.054 |
| 4. | Coated tube 3 | S.S/wire flame | 19.27 | 0.11 | 4.192 |
| 5. | Coated tube 4 | S.S/wire flame | 19.30 | 0.125 | 4.731 |

the Zukauskas correlation (Eq. (3)) are as shown in Fig. 4. The data best fits using method of least squares ($R^2 = 0.96$), Eq. (3), to obtain the following form of the correlation:

$$Nu_\mathrm{d} = 2.095Re_\mathrm{d}^{0.345} \cdot \mathrm{Pr}^{0.37} \cdot \left(\frac{\mathrm{Pr}}{\mathrm{Pr_s}}\right)^{0.25} \quad (6)$$

where all fluid properties are evaluated at the free-stream fluid temperature except for $Pr_s$, which is evaluated at the surface temperature. Considering the fact that the Reynolds No. were much lower than the critical values to account for heat transfer enhancements based on roughness, the $h_l$ values for plain tubes were applicable to the coated tubes.

### 4.2 Pool boiling heat transfer coefficient ($h_{npb}$)

The results obtained for pool boiling heat transfer coefficient on a plain tube surface are plotted in Fig. 5 and compared with the predicted values from different correlations. It was found that the present results were close to those predicted using Gorenflo correlation.

For pool boiling, the data plotted is shown in Fig. 6. The plots are best fit using a straight line function on log–log scale and tabulated in Table 2. The heat transfer coefficient for pool boiling increased with increasing roughness and heat flux. The pool boiling heat transfer coefficient for a surface depends on the nucleation site density. The increased roughness creates more nucleation sites over a wide range of radii than a plain surface thereby generating much larger sized bubbles in a shorter time period and hence increased heat transfer. The enhancements were higher at higher heat flux as it leads to more number of active nucleation sites and a higher rate of bubble generation thereby transferring more heat in the form of latent heat.

The results from Table 2 reveal that there is a maximum enhancement of about 153% for the rougher tube at the heat flux of 45 kW/m$^2$. The comparison of bubble generation from Fig. 7 reveal the effect of higher heat flux on a plain surface versus a rough surface. As evident from the pictures, the rough surface show a much higher concentration of bubble activity on the tube surface at all heat fluxes. Even though there is an increase in heat transfer coefficient with increased heat flux, the increase cannot be continuous as at higher heat flux the generated bubbles start coalescing near the top surface moving along the tube circumference as seen in Fig. 7(c) and (f). The coalescence of bubbles and the formation of large scale bubble slugs on the tube surface may eventually lead to a decrease in heat transfer coefficient as the bubble slug would prevent the access of liquid to the heated surface.

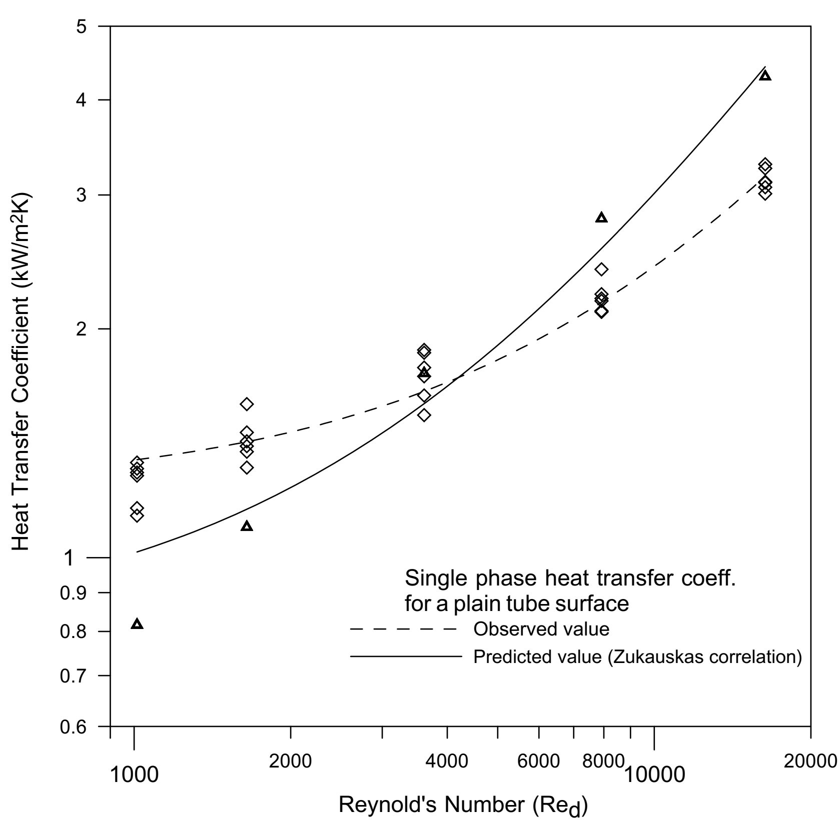


**Fig. 4.** The comparison of experimental results for single-phase heat transfer coefficient ($h_l$) with the predicted values by Zukauskas correlation.

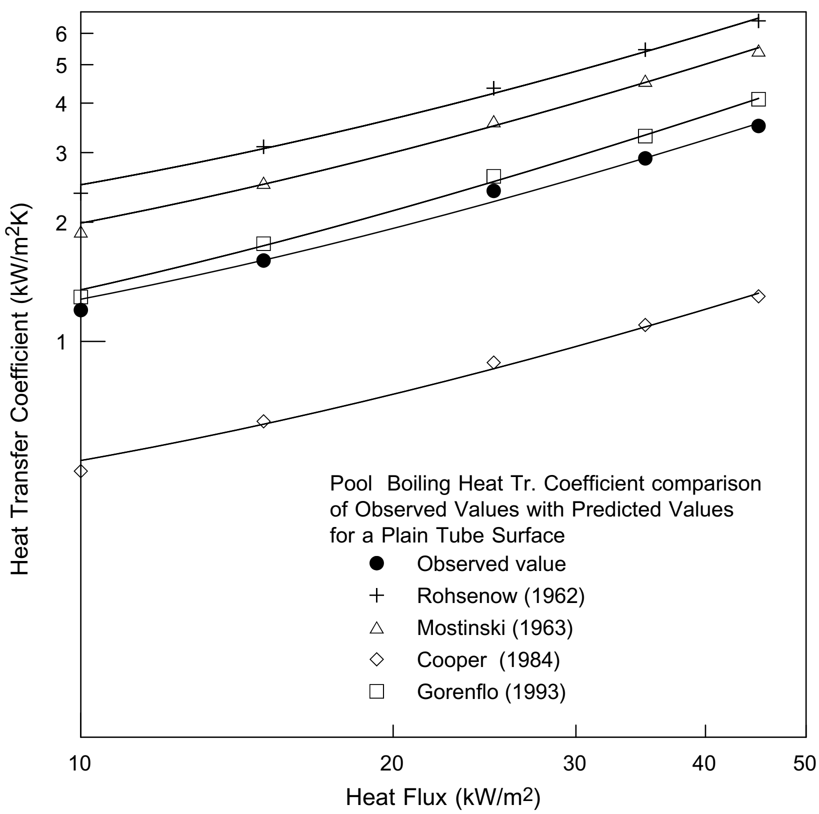


**Fig. 5.** The comparison of the observed value of pool boiling heat transfer coefficient ($h_{npb}$) with the predicted values by different correlations for a plain tube surface.

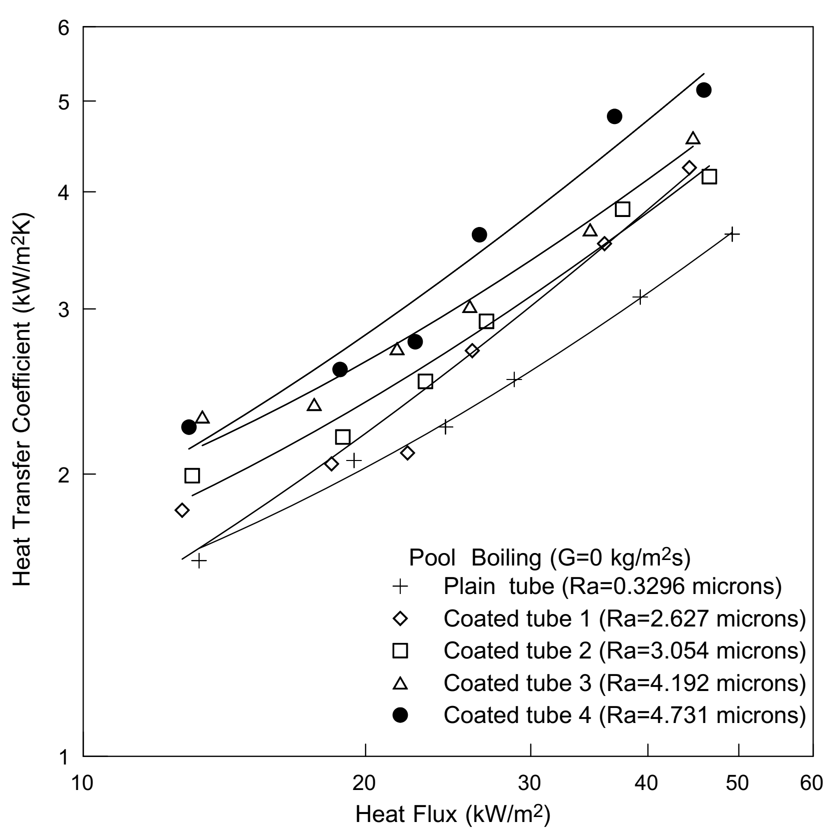


**Fig. 6.** Comparison of pool boiling ($G = 0$ kg/m$^2$ s) heat transfer coefficient for a single tube with different surface roughness.

**Table 2**
Pool boiling enhancements at different heat flux

| Surface type | Heat transfer coefficient (kW/m$^2$ K) based on Fig. 6 | | | | | |
|---|---|---|---|---|---|---|
| | $q$ = 15 kW/m$^2$ | | $q$ = 25 kW/m$^2$ | | $q$ = 45 kW/m$^2$ | |
| | $h_{npb}$ | $h/h_{plain}$ | $h_{npb}$ | $h/h_{plain}$ | $h_{npb}$ | $h/h_{plain}$ |
| Plain tube ($Ra$ = 0.3296 μm) | 1.73 | 1 | 2.35 | 1 | 3.36 | 1 |
| Coated tube 1 ($Ra$ = 2.627 μm) | 1.84 | 1.06 | 2.65 | 1.13 | 4.037 | 1.2 |
| Coated tube 2 ($Ra$ = 3.054 μm) | 2.021 | 1.17 | 2.795 | 1.19 | 4.057 | 1.21 |
| Coated tube 3 ($Ra$ = 4.192 μm) | 2.272 | 1.31 | 3.066 | 1.30 | 4.327 | 1.29 |
| Coated tube 4 ($Ra$ = 4.731 μm) | 2.312 | 1.34 | 3.352 | 1.43 | 5.139 | 1.53 |

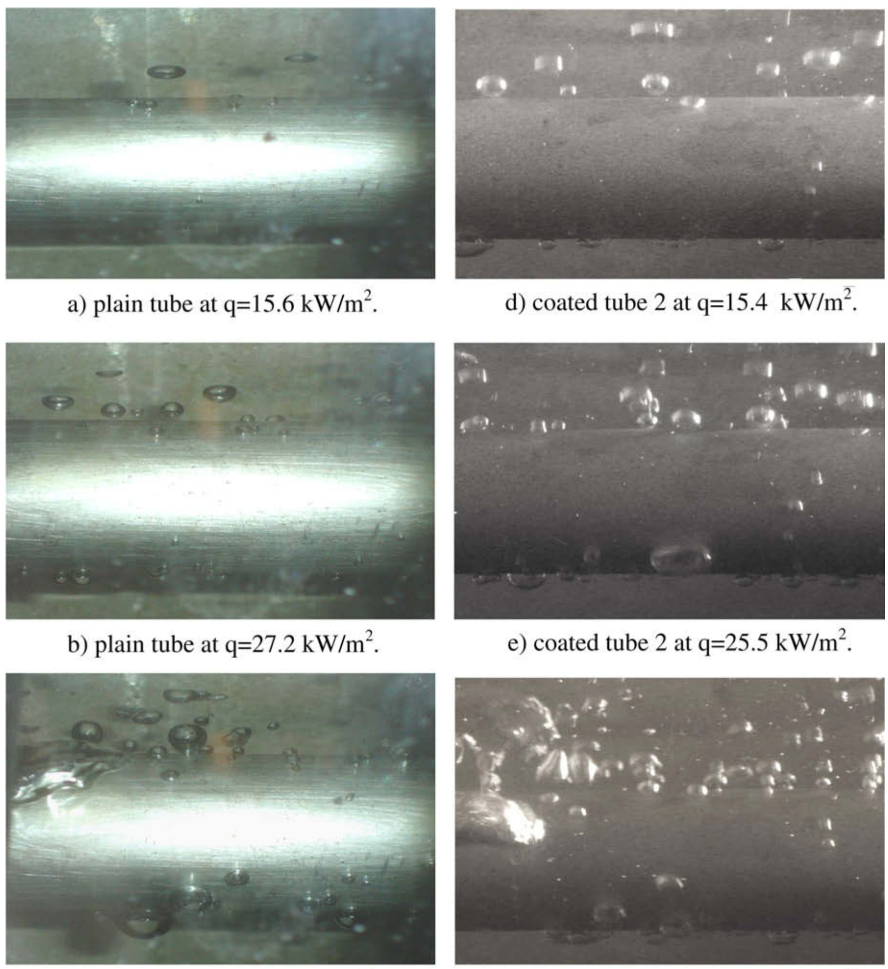
a) plain tube at q=15.6 kW/m$^2$.
d) coated tube 2 at q=15.4 kW/m$^2$.
b) plain tube at q=27.2 kW/m$^2$.
e) coated tube 2 at q=25.5 kW/m$^2$.
c) plain tube at q=48.5 kW/m$^2$.
f) coated tube 2 at q= 42.6 kW/m$^2$.

**Fig. 7.** Comparison of bubble generation between a plain and a coated tube at different heat flux for pool boiling conditions.

The pool boiling data for all the test surfaces in the heat flux range 12–45 kW/m$^2$ were found to fit the following equation incorporating the effect of surface roughness as:

$$h_{npb} = B \cdot q^n \cdot (Ra/d_o)^m \quad (7)$$

where $h_{npb}$, $q$, $Ra$, $d_o$ are in kW/(m$^2$ K), kW/m$^2$, m and m, respectively. The coefficients for the above equation were found to be $B$ = 0.931, $n$ = 0.686, $m$ = 0.123 for the pool boiling data fitted using method of least squares at 95% confidence level and having $R^2$ value of 0.922.

*4.3 Flow boiling heat transfer coefficient (h)*

The effect of cross-flow boiling on heat transfer is as shown in Figs. 8–11 for different mass flux ranging from 16.2 to 258.49 kg/m$^2$ s. The results of flow boiling enhancements are tabulated in Table 3. The influence of mass flux ($G$) on heat transfer coefficient for a plain and a coated tube is shown in Figs. 12 and 13, respectively. The figures show that the effect of cross-flow velocity is relatively more at low heat flux and diminishes with the increase of heat flux.

The results for flow boiling reveal that the increase in flow velocity leads to suppression in nucleation activity and as peak velocities are attained most of the tube surface do not show any nucleation except in the upper surface (which is in the wake region of the flow as seen in Fig. 14) of the tubes which may account for some nominal enhancement. The comparison between plain tube and coated tubes pictures for flow boiling show comparatively enhanced bubble activity for the coated tubes at all the mass fluxes. As observed from Table 3, the coated tubes continue to show

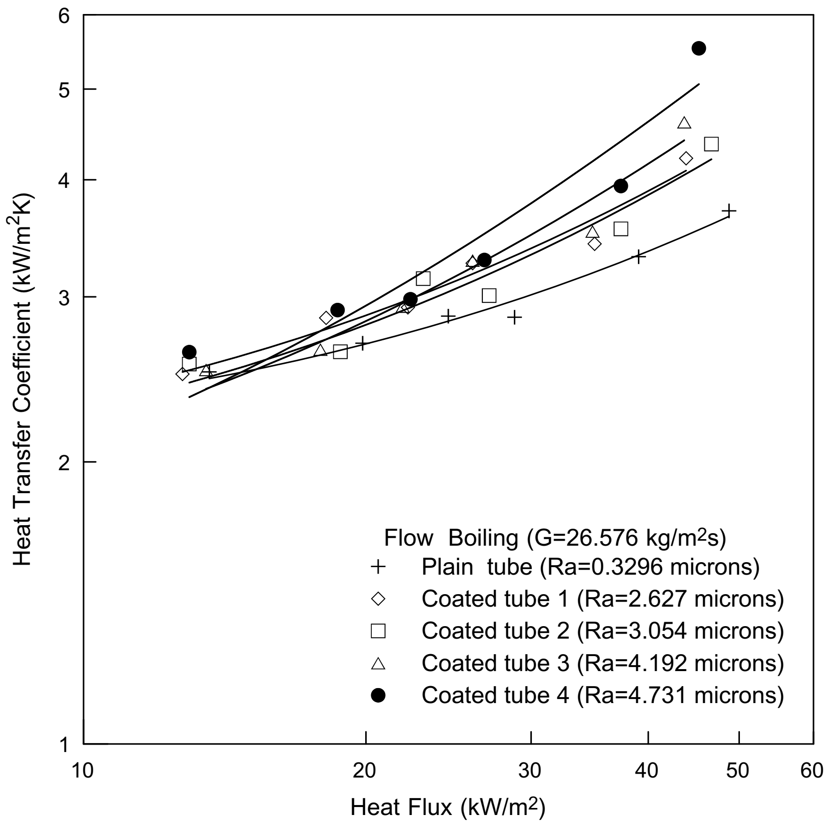


**Fig. 8.** Comparison of flow boiling ($G = 26.576$ kg/m$^2$ s) heat transfer coefficient for a single tube with different surface roughness.

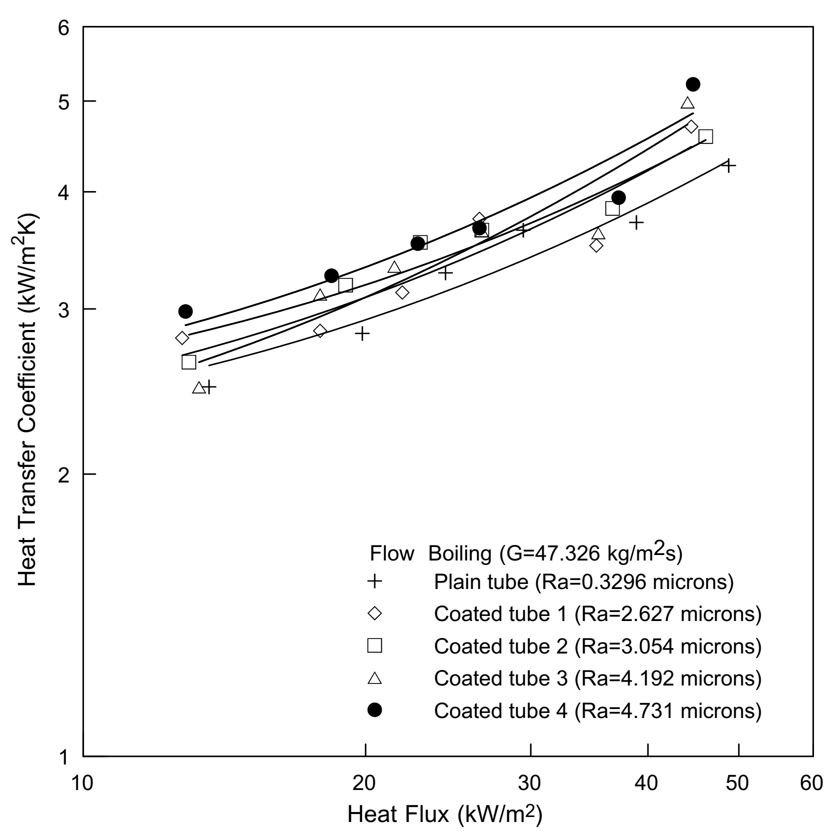


**Fig. 9.** Comparison of flow boiling ($G = 47.326$ kg/m$^2$ s) heat transfer coefficient for a single tube with different surface roughness.

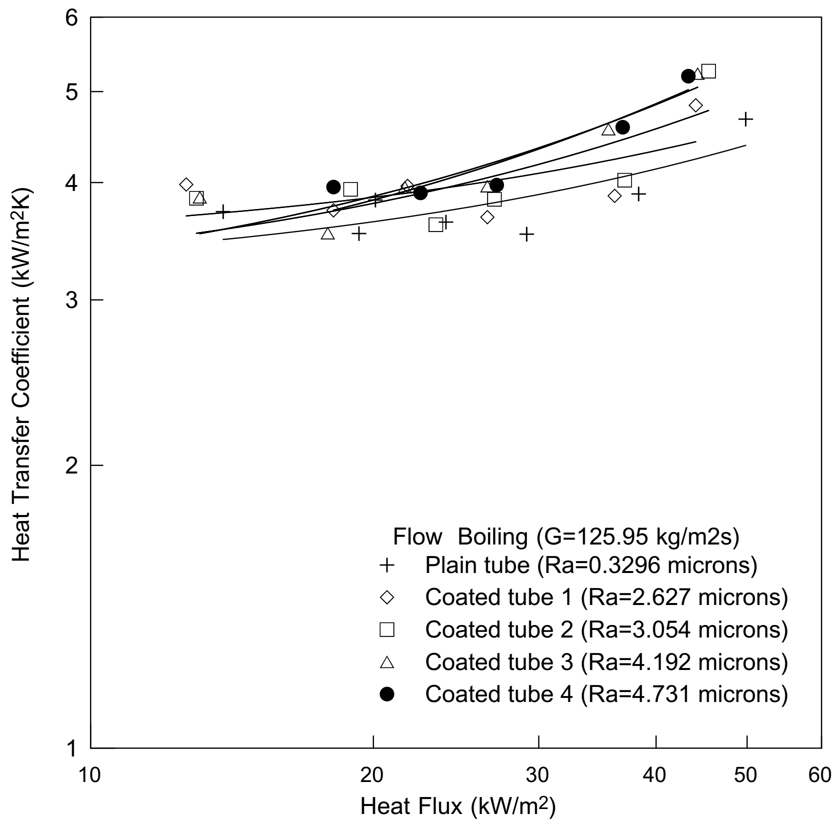


**Fig. 10.** Comparison of flow boiling (125.95 kg/m$^2$ s) heat transfer coefficient for a single tube with different surface roughness.

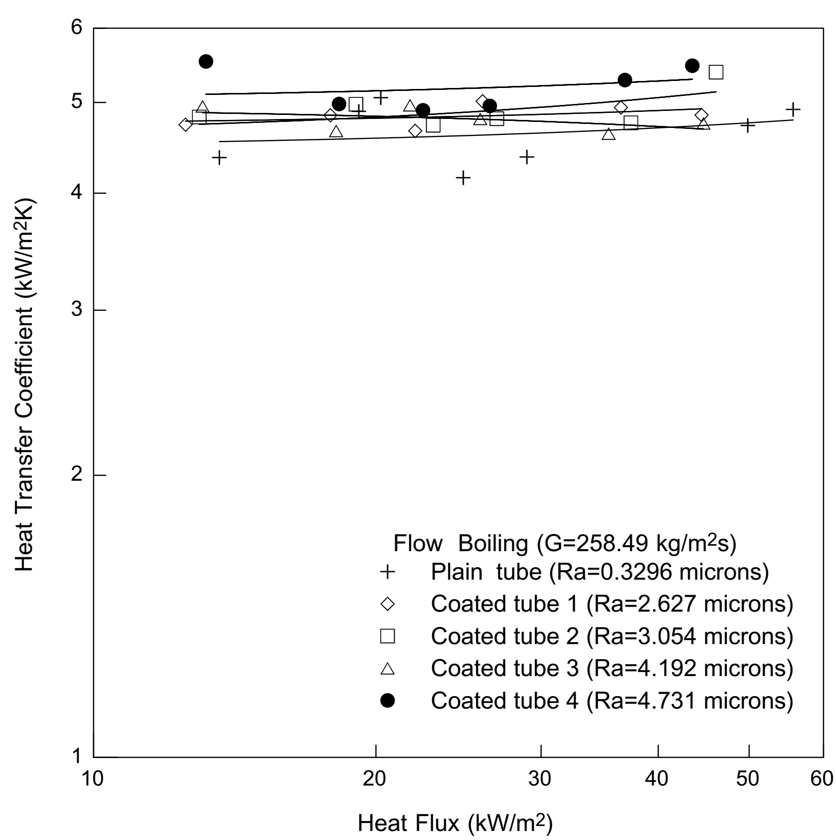


**Fig. 11.** Comparison of flow boiling (258.49 kg/m$^2$ s) heat transfer coefficient for a single tube with different surface roughness.

**Table 3**
Flow boiling enhancements in heat transfer coefficients at different mass flux

| Surface type | Heat transfer coefficient (kW/m$^2$ s) | | | | | | | | | | | | | | | |
|---|---|---|---|---|---|---|---|---|---|---|---|---|---|---|---|---|
| | $G$ = 26.576 kg/m$^2$ s | | | | $G$ = 47.326 kg/m$^2$ s | | | | $G$ = 125.95 kg/m$^2$ s | | | | $G$ = 258.49 kg/m$^2$ s | | | |
| | $q$ = 25 kW/m$^2$ | | $q$ = 45 kW/m$^2$ | | $q$ = 25 kW/m$^2$ | | $q$ = 45 kW/m$^2$ | | $q$ = 25 kW/m$^2$ | | $q$ = 45 kW/m$^2$ | | $q$ = 25 kW/m$^2$ | | $q$ = 45 kW/m$^2$ | |
| | $h$ | $\epsilon$ | $h$ | $\epsilon$ | $h$ | $\epsilon$ | $h$ | $\epsilon$ | $h$ | $\epsilon$ | $h$ | $\epsilon$ | $h$ | $\epsilon$ | $h$ | $\epsilon$ |
| Plain tube | 2.89 | 1 | 3.46 | 1 | 3.22 | 1 | 4.12 | 1 | 3.75 | 1 | 3.97 | 1 | 4.6 | 1 | 4.71 | 1 |
| Coated tube 1 | 3.18 | 1.1 | 4.01 | 1.16 | 3.43 | 1.07 | 4.32 | 1.05 | 4.01 | 1.17 | 4.28 | 1.19 | 4.82 | 1.05 | 4.95 | 1.05 |
| Coated tube 2 | 3.13 | 1.08 | 3.98 | 1.15 | 3.51 | 1.09 | 4.44 | 1.08 | 4.04 | 1.18 | 4.53 | 1.26 | 4.80 | 1.04 | 4.99 | 1.06 |
| Coated tube 3 | 3.22 | 1.11 | 4.31 | 1.25 | 3.49 | 1.08 | 4.65 | 1.13 | 4.11 | 1.20 | 4.74 | 1.31 | 5.04 | 1.09 | 5.07 | 1.07 |
| Coated tube 4 | 3.43 | 1.19 | 4.74 | 1.37 | 3.71 | 1.15 | 4.67 | 1.33 | 4.14 | 1.21 | 4.79 | 1.33 | 5.05 | 1.1 | 5.28 | 1.12 |

$\epsilon = h/h_{\text{plain}}$, enhancement ratio with respect to a plain surface.

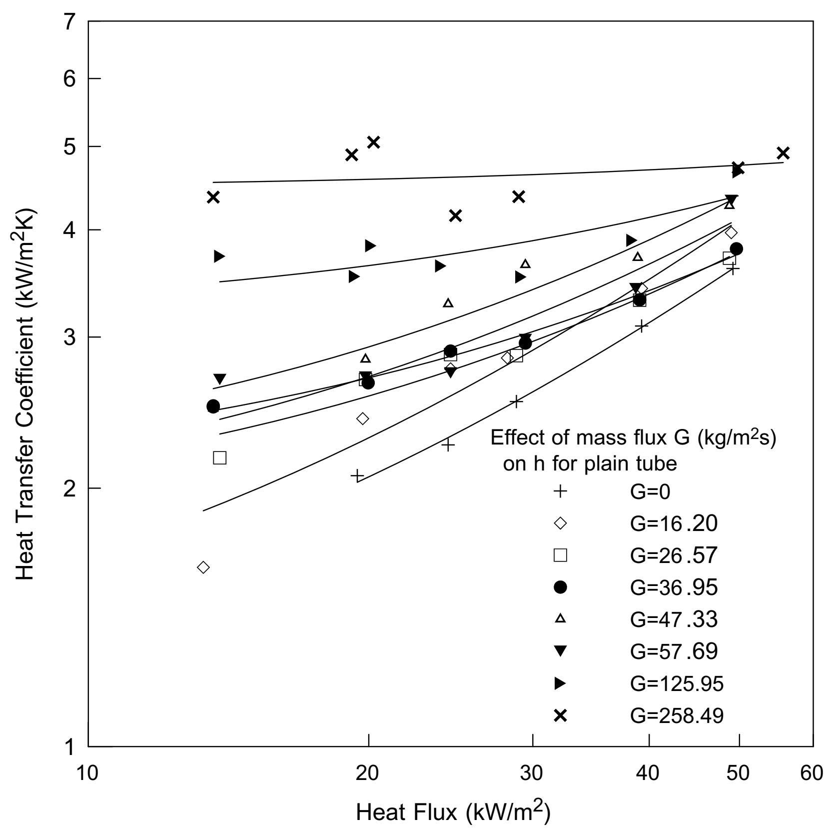


**Fig. 12.** Effect of different cross-flow velocity on boiling heat transfer coefficient for a plain tube.

enhancements (maximum 1.37 times) with the increase in mass flux due to the continued nucleation activity even at high mass flux. However, due to suppression of nucleate boiling at highest mass flux the enhancements in heat transfer coefficient between a plain and a coated tube are reduced (max enhancements at 1.12 for coated tube 4 at a mass flux of 258.49 kg/m$^2$ s).

The circumferential variation of heat transfer coefficient (Fig. 15) for the tubes in pool boiling suggest the lowest values for the upper surface of the tube periphery due to coalescence of bubbles near the top surface while the highest values are near the lower surface of the tube periphery. At higher mass flux, the profile changes as the suppression of boiling at the lower surface reduces the local heat transfer coefficient whereas the wake region has some nucleation leading to nominal enhancements.

The flow boiling data was found to best fit the Kutateladze equation (Eq. (2)) with the value of $n = 2.258$ with the data fitted using the method of least squares at 95% confidence level and having a $R^2$ value of 0.79. Here the liquid phase convection component $h_l$ was calculated using Eq. (6). Thus, Eq. (2) fits the following form:

$$\frac{h}{h_l} = \left[1 + \left(\frac{h_{npb}}{h_l}\right)^{2.258}\right]^{1/2.258} \tag{8}$$

The experimental versus predicted value (based on Eq. (8)) for the flow boiling heat transfer coefficient is shown in Fig. 16. As observed from the figure, most of the observed values were within ±20% from those predicted using Eq. (8).

## 5. Conclusions

1. The increased roughness due to coatings creates more nucleation sites thereby generating much larger sized bubbles in a shorter time period and hence increases heat transfer. The enhancements were higher at higher heat flux as it leads to more number of active nucleation sites and a higher rate of bubble generation.
2. The heat transfer data for plain and coated tubes under pool boiling conditions was found to best fit the equation of the form: $h_{npb} = B \cdot q^n \cdot (Ra/d_o)^m$, where the coefficients

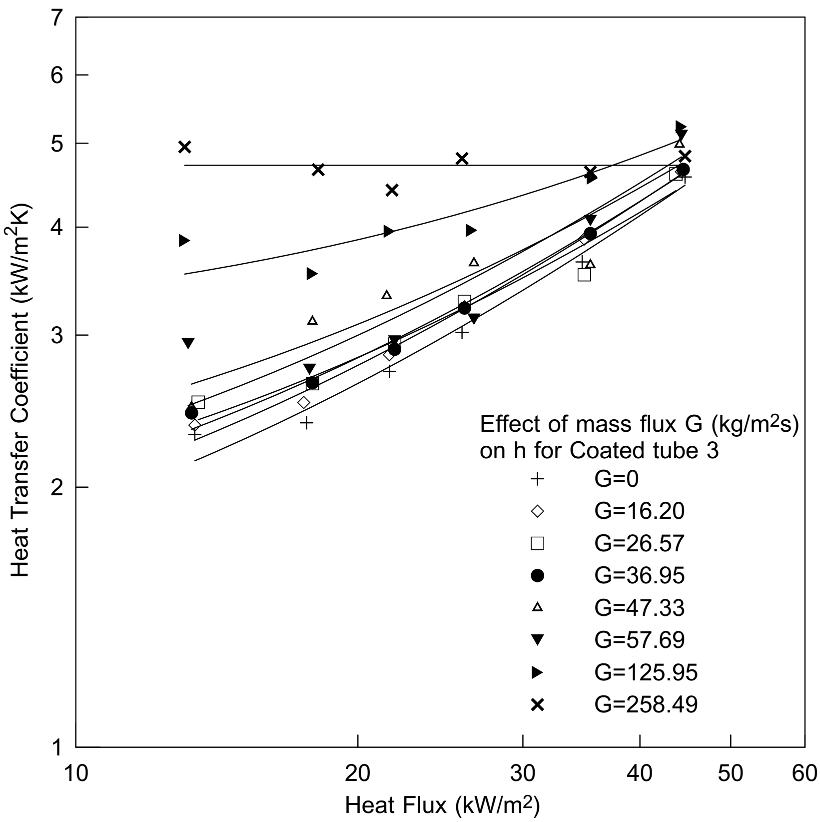


**Fig. 13.** Effect of different cross-flow velocity on boiling heat transfer coefficient for coated tube 3.

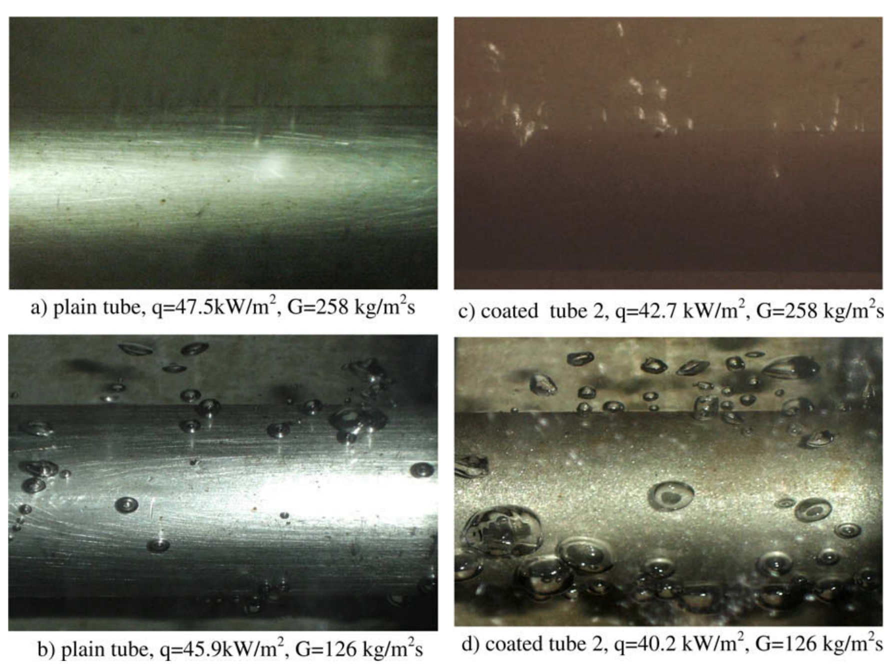


**Fig. 14.** Comparison of bubble generation between a coated tube and a plain tube showing the influence of mass flux.

are $B = 0.931$, $n = 0.686$, $m = 0.123$ and $h_{npb}$, $q$, $Ra$, $d_o$ are expressed in kW/(m$^2$ K), kW/m$^2$, m and m, respectively.

3. The flow boiling data was found to best fit the Kutateladze equation $h = h_l[1 + (h_{npb}/h_l)^n]^{1/n}$ with the value of $n =$ 2.258.

4. The comparison between plain tube and rough tubes (created by coatings) performance for flow boiling show comparatively enhanced bubble activity for the rough tubes at all the mass fluxes. Though the increase in flow velocity leads to a suppression in nucleation activity and as peak velocities are attained most of the tube surface do not

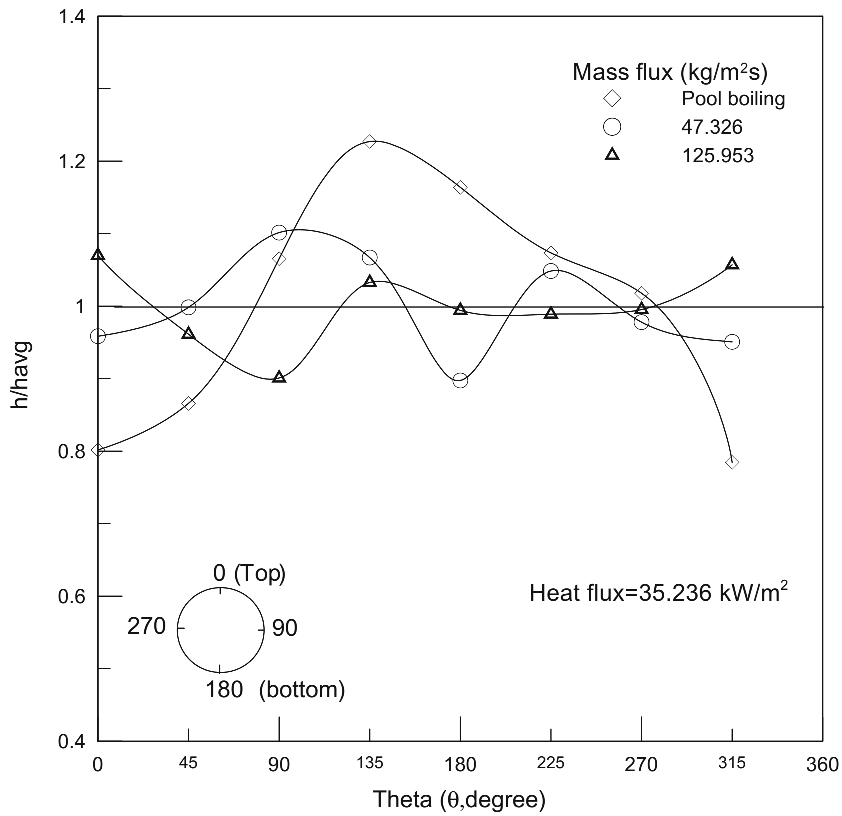


**Fig. 15.** The circumferential variation of heat transfer enhancement for coated tube 4 at different mass flux.

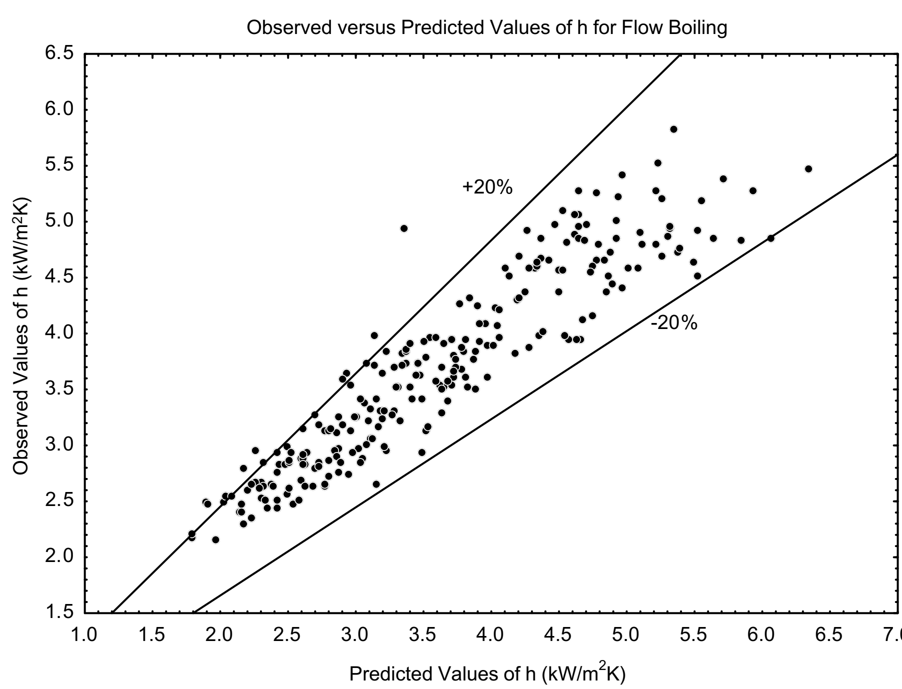


**Fig. 16.** Experimental versus predicted heat transfer coefficient for a single tube in flow boiling.

show any nucleation except in the upper surface(which is in the wake region of the flow) of the rough (coated) tubes which may account for some nominal enhancement in the tube overall heat transfer coefficient.

## References

[1] W.M. Rohsenow, A method of correlating heat transfer data for surface boiling of liquids, ASME J. Heat Transfer 74 (1952) 969–976.

[2] S.T. Hsu, F.W. Schmidt, Measured variations in local surface temperature in pool boiling of water, ASME J. Heat Transfer 83 (1961) 254–260.
[3] I.L. Mostinski, Calculation of heat transfer and critical heat flux in boiling liquids based on the law of corresponding states, Teploenergetika, English Abstract, Brit. Chem. Eng. 8 (8) (1963) 580.
[4] P.J. Marto, W.M. Rohsenow, Effects of surface on nucleate pool boiling of sodium, ASME J. Heat Transfer 88 (1966) 196–204.
[5] R.I. Vachon, G.E. Tanger, D.L. Davis, G.H. Nix, Pool boiling on polished and chemically etched stainless steel surfaces, ASME J. Heat Transfer 90 (1968) 231–238.
[6] M.G. Cooper, Heat flow rates in saturated nucleate pool boiling – a wide ranging examination using reduced properties, Adv. Heat Transfer 16 (1984) 157–239.
[7] J.R. Thome, Nucleate pool boiling of hydrocarbon mixtures on a Gewa-TX tube, Heat Transfer Eng. 10 (1) (1989) 37–44.
[8] R.L. Webb, C. Pais, Nucleate pool boiling data for five refrigerants on plain integral-fin and enhanced tube geometries, Int. J. Heat Mass Transfer 35 (8) (1992) 1893–1904.
[9] D. Gorenflo, Pool Boiling, VDI-Heat Atlas, VDI-Verlag, Dusseldorf, 1993.
[10] M.G. Kang, Experimental investigation of tube length effect on nucleate pool boiling heat transfer, Ann. Nucl. Energy 25 (4–5) (1998) 295–304.
[11] I.L. Pioro, Experimental evaluation of constants for the Rohsenow pool boiling correlation, Int. J. Heat Mass Transfer 42 (1999) 2003–2013.
[12] S. Yilmaz, J.W. Westwater, Effect of velocity on heat transfer to boiling Freon-113, J. Heat Transfer 102 (1980) 26–31.
[13] W.M. Rosenhow, Heat Transfer Associated with Nucleate Boiling, Proceedings of Heat Transfer Fluid Mechanics Institute, Stanford University Press, 1953, p.123.
[14] R.M. Fand, K.K. Keshwani, M.M. Jotwani, R.C.C. Ho, Simultaneous boiling and forced convection heat transfer from a horizontal cylinder to water, J. Heat Transfer 98 (1976) 395–400.
[15] S.S. Kutateladze, Boiling heat transfer, Int. J. Heat Mass Transfer 4 (1961) 31–45.
[16] R.L. Singh, J.S. Saini, H.K. Verma, Effect of cross-flow on boiling heat transfer of refrigerant-12, Int. J. Heat Mass Transfer 28 (2) (1985) 515–517.
[17] A. Zukauskas, J. Karni, High Performance Single-phase Heat Exchangers, Hemisphere Publishing Corporation, 1989. pp. 207–238.
[18] A.A. Zukauskas, J.J. Ziugzda, Heat Transfer of a Cylinder in Cross-flow, Hemisphere Publishing Corporation, 1985.
[19] A. Gupta, J.S. Saini, H.K. Varma, Boiling heat transfer in small horizontal tube bundles at low cross-flow velocities, Int. J. Heat Mass Transfer 38 (4) (1995) 599–605.
[20] S.J. Kline, F.A. McClintock, Describing uncertainties in single-sample experiments, Mech. Eng. (1953) 3.